Vol. 81, No. 2

Varicella-Zoster Virus Infection of Human Fibroblast Cells Activates the c-Jun N-Terminal Kinase Pathway[▽]

Heidi J. Zapata,[1] Masako Nakatsugawa,[2] and Jennifer F. Moffat[1]*

Department of Microbiology and Immunology[1] and Department of Cell and Developmental Biology,[2] State University of New York Upstate Medical University, 750 E. Adams Street, Syracuse, New York 13210

The transcription factors ATF-2 and c-Jun are important for transactivation of varicella-zoster virus (VZV) genes. c-Jun is activated by the c-Jun N-terminal kinase (JNK), a member of the mitogen-activated protein kinase pathway that responds to stress and cytokines. To study the effects of VZV on this pathway, confluent human foreskin fibroblasts were infected with cell-associated VZV for 1 to 4 days. Immunoblots showed that phosphorylated JNK and c-Jun levels increased in VZV-infected cells, and kinase assays determined that phospho-JNK was active. Phospho-JNK was detected after 24 h, and levels rose steadily over 4 days in parallel with accumulation of VZV antigen. The two main activators of JNK are MKK4 and MKK7, and levels of their active, phosphorylated forms also increased. The competitive inhibitor of JNK, SP600125, caused a dose-dependent reduction in VZV yield (50% effective concentration, $\cong 8$ μM). Specificity was verified by immunoblotting; phospho-c-Jun was eliminated by 18 μM SP600125 in VZV-infected cells. Immunofluorescent confocal microscopy showed that phospho-c-Jun and most of phospho-JNK were in the nuclei of VZV-infected cells; some phospho-JNK was in the cytoplasm. MKK4, MKK7, JNK, and phospho-JNK were detected by immunoblotting in purified preparations of VZV virions, but c-Jun was absent. JNK was located in the virion tegument, as determined by biochemical fractionation and immunogold transmission electron microscopy. Overall, these results demonstrate the importance of the JNK pathway for VZV replication and advance the idea that JNK is a useful drug target against VZV.

Cells monitor their environments through surface receptors, transmitting signals from the surroundings and responding appropriately in terms of gene expression. It is known that cells respond to environmental cues, growth factors, and stress by the activation of mitogen-activated protein kinases (MAPKs), thus making these pathways main regulators of the intracellular environment. MAPKs are commonly activated through a three-tiered phosphorylation cascade (9, 30). A stimulus at the plasma membrane leads to sequential activation of MAP3Ks (MAP kinase kinase kinase; usually a serine/threonine-specific kinase), which next activate MAP2Ks (S/T and tyrosine dual specific kinase), which then activate MAPKs by phosphorylation of a TXY motif in the activation loop. Activated MAPKs translocate to the nucleus and phosphorylate transcription factors, creating a direct link between outside cues and changes in gene expression in the nucleus. MAPKs also have roles in the cytoplasm, where they may influence apoptosis and other functions. The three best-characterized signaling cascades are known by their MAPKs: extracellular signal-regulated kinase (ERK), c-Jun N-terminal kinase (JNK), and p38 kinase (9). The JNK pathway is one of the most complex, mediating responses to osmotic stress, UV radiation, inflammation, growth factors, and apoptosis (31, 59). Following engagement of cellular receptors, the signals are first transmitted through Rho family GTPases (12, 30, 50) or other unknown intermediates

and at least 13 known MAP3Ks (31). Scaffold proteins coordinate the propagation of the stimuli to the JNK-specific MAP2Ks, MKK4/MEK4 and MKK7/MEK7 (52), both of which are required to activate the three isoforms of JNK. Dual phosphorylation on the TPY amino acid motif (13) by MKK4 and MKK7 is necessary to activate JNK (43, 48). The main substrate of JNK is c-Jun, a member of the heterodimeric AP-1 transcription factor family (13, 32), which is phosphorylated by JNK at serines 63 and 73 (41).

Viruses have coevolved with their human hosts and so have adapted to the intricacies of signaling networks by manipulating the MAPK pathways to favor viral replication (22). Widely diverse families of viruses activate MAPKs upon binding, entry, or replication (22). To mention only a small segment of the field, influenza virus, human hepatitis viruses, and herpesviruses have evolved strategies to modulate MAPKs for oncogenic transformation, to prevent apoptosis, and to activate transcription factors (11, 18, 46, 56). Although the purpose of MAPK activation is difficult to discern and is unique to each virus, there appears to be a common requirement for induction of transcription factors that regulate viral and cellular gene expression.

Interaction with the JNK pathway to modulate the intracellular environment is likely beneficial at many stages of herpesvirus infection. Kaposi's sarcoma-associated herpesvirus encodes the viral kinase ORF36 (open reading frame 36), which phosphorylates and activates JNK, and inhibition of JNK blocks viral gene expression at late stages of infection (23). Kaposi's sarcoma-associated herpesvirus activates JNK and AP-1 in endothelial cells at the entry stage, and JNK inhibitors or dominant-negative proteins block infectivity (55). It is well established that Epstein-Barr virus encodes two membrane

---

* Corresponding author. Mailing address: Department of Microbiology and Immunology, State University of New York Upstate Medical University, 750 E. Adams St., Syracuse, NY 13210. Fax: (315) 464-4417. Phone for J. F. Moffat: (315) 464-5454. E-mail: moffatj@upstate.edu.

proteins, LMP-1 and -2, that activate JNK, causing increases in c-Jun and AP-1 activity (8, 17, 33). Herpes simplex virus type 1 (HSV-1) infection activates JNK and p38 soon after entry and maintains activation for as long as 14 h (49). The JNK pathway can be activated by external addition of HSV-1 glycoprotein H (gH) peptides (20) or expression of the immediate-early protein ICP27 (24). HSV-1 also activates JNK and c-Jun in cultured rat neurons and in patients with HSV-associated acute focal encephalitis (58). Varicella-zoster virus (VZV) infection has been found to activate the JNK and p38 pathways in melanoma cells (62), and inhibition of JNK led to a twofold increase in VZV replication. Stable expression of VZV ORF61 alone in MeWo cells was linked to phosphorylation of JNK, and sustained JNK activation reduced the VZV yield in this system (61). Conversely, we report here that VZV replication in confluent human foreskin fibroblasts (HFFs) is dependent on JNK activity.

VZV is a human-restricted alphaherpesvirus that infects nondividing cells such as epithelial cells, dermal fibroblasts, memory T cells, and neurons (1). This pattern of tissue and cell tropism is reflected in the diseases caused by VZV, which are chicken pox (varicella) upon primary infection and shingles (herpes zoster) upon reactivation from latency in dorsal root ganglia. In cultured human skin fibroblast cells, VZV grows well even when the monolayers are confluent (44). In these contact-inhibited fibroblasts, VZV infection selectively activates cyclin-dependent kinases that are involved in regulating cell division (44). This atypical cellular environment is apparently important for VZV, since cyclin-dependent kinase inhibitors such as roscovitine and purvalanol prevent replication (68). The regulation of the cell cycle is linked to MAPKs (47, 66), although little is known about their roles in VZV-infected quiescent skin fibroblasts, which are primary cells with normally regulated signaling cascades.

Transcription factors, both cellular and viral, act in concert to stimulate VZV gene expression. VZV ORFs 4, 10, 61, 62, and 63 encode known transactivators that interact with cellular transcription factors including Oct-1, TATA binding protein, USF, Sp1, activating transcription factor 2 (ATF-2), AP-1, and certainly others (57, 60, 63). For example, the host cell factor 1 protein (HCF-1) is necessary for the ORF10 protein and immediate-early protein 62 (IE62) to synergize at the ORF62 promoter (53). Many recognition sites for AP-1/TRE (TPA [12-O-tetra-decanoyl phorbol 13-acetate] response element) and ATF/cis-acting replication element sites are found in VZV promoters, and knocking down c-Jun and ATF-2 (components of AP-1) with antisense RNA reduced the transcription of VZV genes (64). The JNK pathway is directly upstream of c-Jun and is the main activator of the transcription factor (13). The key role of AP-1 transcription factors in VZV gene expression led us to hypothesize that the JNK pathway is manipulated by the virus in resting fibroblasts.

Here we report that three levels of the JNK pathway were activated following VZV infection of confluent human foreskin fibroblasts. A large increase in JNK activity was associated with phosphorylation of its activators, MKK4 and MKK7, and with phosphorylation of its substrate, c-Jun. The activation of the JNK pathway was sustained, and the levels of phosphorylated JNK increased concurrently with the spread of VZV over 4 days. The JNK and c-Jun proteins were found in the nuclei of infected cells, where they could transactivate viral gene expression. Some phosphorylated JNK was also found in the cytoplasm, where it could be involved in later stages of replication such as tegumentation and rearrangements of the cytoskeleton. Indeed, JNK was associated with purified VZV virions. Chemical inhibition of JNK caused a dose-dependent reduction in virus spread, further emphasizing the importance of this signaling pathway to VZV replication and advancing the idea that JNK is a useful drug target against VZV.

MATERIALS AND METHODS

Cells and viruses. HFFs (cATCC no. CCD-1137Sk) and MeWo cells, a human melanoma cell line (a gift of Charles Grose, University of Iowa), were maintained in Eagle minimal essential medium with Earle's salts and L-glutamine, supplemented with 10% heat-inactivated fetal calf serum, penicillin-streptomycin (5,000 IU/ml), amphotericin B (250 μg/ml), and nonessential amino acids. The MeWo MPR-KD cell line (7), which is deficient in the mannose 6-phosphate receptor (a gift of Michael and Anne Gershon, Columbia University), was maintained in supplemented tissue culture medium with 2 μg of puromycin (Sigma)/ml. All media and supplements were obtained from Cellgro/Media Tech (Washington, DC). Cells were grown to confluence at 37°C in humidified 5% CO$_2$. The VZV recombinant parental Oka strain (rPOKA) (54) was propagated by passage of infected cells showing cytopathic effect onto uninfected monolayers of HFFs.

Kinexus Western blot array. Confluent layers of HFFs were either mock infected or VZV infected for 3 days under 10% or 1% serum conditions. Infection consists of adding infected cells to uninfected cells. Mock infection consists of the addition of uninfected cells. Cell lysates were then collected using the Kinexus lysis buffer (20 mM Tris [pH 7], 2 mM EGTA, 5 mM EDTA, 30 mM sodium fluoride, 40 mM glycerophosphate, 10 mM sodium pyrophosphate, 2 mM sodium orthovanadate, 10 μM leupeptin, 5 μM pepstatin A, 0.5% Triton X-100, and protease inhibitors [Roche, Indianapolis, IN]). The cells were sonicated twice for 15 s to rupture the cells. The homogenate was then subjected to ultracentrifugation at 100,000 × g for 30 min on a Beckman TL-100 tabletop ultracentrifuge. The lysates were then diluted in sodium dodecyl sulfate-polyacrylamide gel electrophoresis (SDS-PAGE) sample buffer and sent to Kinexus (Vancouver, British Columbia, Canada) for analysis using Kinetworks phosphosite screen 1.3. This screen analyzed 31 phosphorylation sites in phosphoproteins. Kinetworks protein kinase screen 1.2 was also performed under 1% serum conditions. This screen analyzed total levels of 75 proteins.

Antibodies and inhibitors. Antibodies to phospho-JNK (44-682G) and JNK 1 (anti-JNK 1 pan, 44-690G) were purchased from Biosource (Camarillo, CA). Antibodies to phospho-c-Jun (06-659) and total c-Jun (06-225) were purchased from Upstate Biotechnology (Lake Placid, NY). Antibodies to phospho-JNK (sc-6254) were purchased from Santa Cruz (Santa Cruz, CA). Antibodies to total MKK4 (9152), phospho-MKK4 (9156), total MKK7 (4172), and phospho-MKK7 (4171) were purchased from Cell Signaling (Danvers, MA). Polyclonal rabbit antibodies to the VZV proteins IE62, ORF4, and ORF29 were kindly provided by Paul Kinchington of the University of Pittsburgh. Human anti-VZV serum was kindly provided by Ann Arvin of Stanford University. The monoclonal antibody to glycoprotein gE (3B3) was kindly provided by Charles Grose of the University of Iowa. The JNK inhibitor SP600125 was purchased from Biomol (Plymouth Meeting, PA). Stock solutions of 10 mM SP600125 were dissolved in dimethyl sulfoxide (DMSO), aliquoted, and stored at −20°C. The inhibitor was diluted in tissue culture medium for use.

Immunoblotting. Confluent monolayers of HFFs were either mock infected or VZV infected for 3 to 4 days. Cells were also treated with anisomycin (250 ng/ml) for 30 to 40 min as a positive control. Cells were washed with cold phosphate-buffered saline (PBS), and cell lysates were then collected using radioimmunoprecipitation assay (RIPA) buffer (50 mM Tris-HCl [pH 7.4], 1% NP-40, 150 mM NaCl, 1 mM EDTA, 1 mM NaF, 1 mM Na$_3$VO$_4$, and protease inhibitors [Roche]). Lysates were rocked at 4°C for 4 h, sonicated twice for 15 s, and centrifuged at 16,300 × g for 25 min at 4°C, and aliquots were stored at −80°C. For SDS-PAGE, lysates were diluted in sample buffer, boiled at 95°C for 5 min, and then run on 4 to 12% gradient Tris-glycine gels (Cambrex, Rockland, ME). Proteins were transferred to a polyvinylidene difluoride membrane and probed for the respective proteins. The manufacturers' recommended conditions for blocking and probing were used for each antibody. All primary antibodies were used at a 1:1,000 dilution. Either alkaline phosphatase- or horseradish peroxidase-conjugated secondary antibodies were used (Jackson ImmunoResearch).

Signals were detected using Lumi-phos (Pierce, Rockford, IL) or ECL plus (Amersham Biosciences, Piscataway, NJ).

JNK kinase assays. JNK kinase assays were carried out as described in reference 71. Briefly, cell lysates in RIPA buffer were incubated overnight at 4°C on a rocker with 2 μg of c-Jun fusion protein beads (Cell Signaling). The c-Jun protein is expressed as a recombinant protein fusion of c-Jun codons 1 to 89 and glutathione S-transferase (GST). These beads selectively bind JNK and serve as its substrate. The beads were washed once with RIPA buffer and twice with kinase assay buffer (25 mM HEPES [pH 7.4], 25 mM sodium β-glycerophosphate, 25 mM MgCl$_2$, 0.1 mM sodium vanadate, 0.5 mM dithiothreitol). Beads were incubated with kinase assay buffer and 10 μCi of [γ-^{32}P]ATP for 30 min at 30°C. JNK 1α1/stress-activated protein kinase 1c (SAPK 1c) active kinase (4 μg) (Upstate) was used as a positive control. The reaction was terminated by addition of SDS-PAGE sample buffer, and the reaction product was boiled for 5 min at 95°C. The eluted proteins were run on 4 to 12% gradient Tris-glycine gels (Cambrex). The gel was dried, and phosphorylation of the c-Jun substrate was determined by autoradiography.

Immunofluorescence confocal microscopy. HFFs were grown to confluence on glass chamber slides (Nalge Nunc, Naperville, IL) and then either mock infected or VZV infected for 24 to 48 h. The cells were washed twice with CSK buffer (1 M HEPES, 600 mM sucrose, 1.5 M NaCl, 300 mM MgCl$_2$, 1 μg/ml pepstatin, 1 M NaF, 50 mM Na$_3$VO$_4$, 1 M dithiothreitol, protease inhibitors [Roche]), fixed in 10% paraformaldehyde in PBS for 10 min, and then fixed in 100% methanol for 15 min. To avoid autofluorescence, cells were treated with 10% sodium borohydride in PBS for 15 min. Cells were blocked in 10% goat serum–3% bovine serum albumin in Tris-buffered saline and were subsequently stained with a rabbit polyclonal phospho-JNK antiserum, a phospho-c-Jun antiserum, a monoclonal phospho-JNK antiserum (1:100), a human anti-VZV antiserum (kindly provided by Ann Arvin, Stanford University) (1:500), or an IE62 antiserum (generously provided by Paul Kinchington, University of Pittsburgh). Finally, secondary antibodies (1:200) conjugated to rhodamine or fluorescein isothiocyanate (Jackson ImmunoResearch, West Grove, PA) were added. The slides were mounted with Prolong Gold (Molecular Probes, Eugene, OR), and images were collected with a Bio-Rad (Hercules, CA) Lasersharp Plus imaging system.

NR cytotoxicity assay. The neutral red (NR) cytotoxicity assay was performed according to previously described methods (2). NR (Sigma) was diluted in tissue culture medium to 25 μg/ml and incubated overnight at 37°C. Prior to use, the NR solution was filtered (pore size, 0.22 μm) to remove fine dye crystals. HFF cells were seeded on 96-well plates and treated with either 5.0 ng of staurosporine or 0 to 40 μM SP600125. After 0, 24, and 48 h, the medium was removed from the HFF cells and replaced with 0.25 ml of NR solution, and the mixture was incubated for 2 h at 37°C. Cells were then washed and fixed with 0.5% formalin in Dulbecco's PBS with Ca^{2+} and Mg^{2+} (Mediatech). The NR dye that had been taken up by viable cells was extracted with 0.1 ml of desorb solution (1% glacial acetic acid, 50% ethanol). The plate was agitated on an orbital shaker for 25 min, and then the absorbance was read at 540 nm on a microtiter plate spectrophotometer.

Dose-response studies. Cells were grown in 24-well plates to confluence. Cells were pretreated with 0 to 40 μM SP600125 for 45 min. These cells were then infected with cell-associated VZV at a dilution of 1:50 to 1:100. Cells were incubated with increasing doses of SP600125 (0 to 40 μM) and equalized amounts of diluent (DMSO) for 48 h. Drugs were refreshed every 24 h. The yield of VZV infection was determined by a plaque assay. At 0 and 48 h postinfection, cells were trypsinized. Two wells for each dose were titered onto monolayers of MeWo cells in 24-well plates. The titer plates were incubated for 5 to 7 days, then fixed with 3.7% formaldehyde in PBS for 20 min, and finally stained with crystal violet for 10 min. Plaques and syncytia were counted under a dissecting microscope. PFU per milliliter were calculated and plotted against the dose.

Virion purification. Virus particles were purified from VZV-infected MeWo MPR-KD cells as described previously (36, 39). VZV-infected cells (12 to 15 175-cm^2 flasks) showing 80% cytopathic effect were scraped, pelleted by low-speed centrifugation, and subsequently used to make cell extracts by Dounce homogenization in serum-free medium. Nuclei and cell debris were pelleted by low-speed centrifugation and subsequently discarded. The cell extracts were then combined with the infected-cell medium and subjected to high-speed centrifugation (71,000 × g for 2 h at 4°C) to pellet released material and virus particles. The virion pellet was then resuspended in serum-free medium and allowed to sit overnight at 4°C. The next day, the sample was briefly sonicated and subjected to low-speed centrifugation to remove debris. The supernatant was then centrifuged on a 5 to 15% Ficoll gradient (Sigma) for 2 h at 35,000 × g and 4°C. A light-diffusing band migrating approximately halfway down the gradient was extracted, diluted in serum-free medium, and pelleted by centrifugation at

160,000 × g for 1 h at 4°C. The virion preparation was then resuspended in serum-free medium (200 μl) and stored at −80°C. The virion preparation was then analyzed by immunoblotting, and the blot was probed with the appropriate antibodies. Virion purity was determined by probing for the absence of the 130-kDa protein ORF29, the single-stranded DNA binding protein, with a polyclonal antibody.

Electron microscopy. Purified virions were negatively stained with 1% uranyl acetate, by a procedure similar to that described in reference 15, on ultrathin, 400-mesh, carbon type-A grids (Ted Pella, Redding, CA). Formvar was removed from the carbon grids with chloroform, and then a drop (5 μl) of the virion suspension was adsorbed to the grid for 1 min. Excess suspension was removed with filter paper. The grid was washed with water and then covered with a drop of 1% uranyl acetate for 1 min. Excess stain was removed with filter paper. The grid was dried and subsequently viewed by transmission electron microscopy (TEM) (Tecnai 12 Bio Twin, images captured by a Kodak ES4.0 Advantage Plus digital charge-coupled device system 2Kx 2K camera [AMT, Danvers, MA].

For immunogold TEM, VZV- and mock-infected cells were grown as described above, harvested after 4 days by scraping cells into their own media, pelleted, and washed in cold PBS. The cell pellets were overlaid with 1% agarose and then fixed in 3% paraformaldehyde–0.1% glutaraldehyde–1% tannic acid–0.05 M phosphate buffer (pH 6.8) for 2 h at room temperature. The pellets were washed with 0.05 M phosphate buffer, treated with 0.05 M ammonium chloride for 30 min at room temperature, and then washed with water. The pellets were then treated with 0.1% osmium tetroxide for 30 min, rinsed with water, and successively dehydrated in 30%, 50%, 70%, 80%, and 90% ethanol twice for 10 min each time and in 100% ethanol three times for 10 min each time. LR Gold resin in 100% ethanol (1:1) (Electron Microscopy Sciences, Hatfield, PA) was added to the pellets for 1 h at room temperature; it was then replaced with LR Gold containing 0.2% benzyl, and the pellets were incubated overnight at 4°C. Fresh LR Gold with 0.2% benzyl was added for a second overnight incubation at 4°C. The resin was polymerized by exposure to UV light for 5 days at 4°C. Thin sections (thickness, 80 nm) were made with a microtome (Ultracut E; Reichert-Jung), and placed on Formvar-carbon-coated 200-mesh gold grids (Electron Microscopy Sciences). The grids were washed with PBS, incubated in 0.1 M glycine for 30 min, and again washed in PBS. The grids were blocked in 4% bovine serum albumin–0.1% fish gelatin–0.05% Tween 20 solution for 2 h at 4°C and then incubated with an anti-JNK antibody (1:40) or rabbit immunoglobulin G in blocking buffer overnight at 4°C. The grids were then washed with PBS and incubated in a goat anti-rabbit antibody conjugated to 10-nm-diameter gold particles (Electron Microscopy Sciences) for 90 min. The grids were washed with PBS, incubated in 2% glutaraldehyde for 15 min; washed in water, treated with 1% osmium for 30 min, washed extensively in water, and finally stained with 4% uranyl acetate and a lead citrate solution for 15 min each. The grids were rinsed, dried, and subsequently viewed with a Jeol (100S) transmission electron microscope.

Virion detergent and protease treatments. The detergent and protease treatments were modified from methods described previously (73). Purified virions were treated with 1% Triton X-100 alone for 30 min at 37°C, followed by a 1-h centrifugation at 70,000 × g. The supernatant (viral envelope proteins) was precipitated with acetone and resuspended in sample buffer for SDS-PAGE analysis. The pellet (virus particles) was also resuspended in sample buffer for SDS-PAGE. Purified virions were also treated either with trypsin (0.1 mg/ml) alone for 15 min or with trypsin (0.1 mg/ml) and 1% Triton X-100 for 5 or 15 min at 37°C. Proteolysis was terminated by the addition of soybean trypsin inhibitor (0.5 mg/ml) and 0.4 mM phenylmethylsulfonyl fluoride. Proteins were precipitated with acetone, resuspended in sample buffer, and separated by SDS-PAGE.

RESULTS

VZV activates the JNK pathway. Our first approach to determining the signaling status of the cell upon infection with VZV was to use the Kinexus Western blot array. Kinexus provides a service to analyze the expression and phosphorylation states of many protein kinases and cell signaling proteins through the application of specific antibody probes to lysates of infected and uninfected cells. HFFs were used throughout this study, because they are primary cells with unaltered signaling networks, in contrast to oncogenically transformed and immortalized cell lines, which may contain unidentified defects in these pathways. Parallel cultures of HFFs grown in media

TABLE 1. Kinexus Western blot array[a]

Kinase	Phospho epitope	Fold change in protein level at the indicated serum concn		
		Phosphoprotein		Total protein (1% serum)
		10% Serum	1% Serum	
JNK (47 kDa)	T183/Y185	40.15	74.84	1.17
JNK(39 kDa)	T183/Y185	2.22	3.23	0.27
c-Jun	S73	1.84	2.39	$\emptyset$[b]
PKR	T451	10.07	4.1	$\emptyset$[b]

[a] HFF cells were either mock infected or infected with VZV-for 3 days under 10% and 1% serum conditions. Lysates were then collected and used for a Kinexus Western blot array. The n-fold change in phosphorylation or in the total protein amount was calculated as (counts per minute for VZV-infected cells)/(counts per minute for mock-infected cells) from immunoblot densitometry.

[b] $\emptyset$, experiment not done.

containing either 10% or 1% fetal bovine serum were either mock infected (uninfected HFFs) or infected with VZV (cell-associated inoculum) for 3 days, the time point when the maximal VZV titer is achieved, as determined by previous studies (44). Whole-cell extracts were collected and shipped to Kinexus for analysis by immunoblotting. Densitometry of the protein bands was used to calculate the n-fold change in phosphoprotein levels in VZV-infected cells compared to mock-infected cells; it revealed large changes in the phosphorylation of particular proteins (Table 1). The phospho form of protein kinase RNA-activated (PKR), which is activated by phosphorylation in response to viral infection, increased 4- to 10-fold. The 47-kDa isoform of JNK showed 40- to 75-fold-increased phosphorylation levels with serum concentrations of 10% and 1%, respectively. The 39-kDa JNK isoform showed two- to threefold-increased phosphorylation. Phosphorylation of c-Jun, a substrate of JNK, increased approximately twofold with both serum concentrations. To determine whether changes in protein expression levels could account for the observed increases in phosphorylation, Kinexus performed a total-quantity analysis on a broad array of cell proteins. The levels of total JNK increased approximately 0.3- to 1.2-fold, an order of magnitude less than the increase in the phosphorylation of the same protein in VZV-infected HFFs. No proteins tested changed more than twofold (data not shown). The c-Jun protein was not included on the total-protein array, but it was part of the next set of experiments to confirm the Kinexus results by evaluating the individual components of the JNK pathway.

The copious increase in JNK phosphorylation in VZV-infected cells merited further investigation. To explore the phosphorylation status of JNK and other members of its pathway, paired sets of antibodies to total and phosphorylated forms were used in separate immunoblots. Because the JNKs are encoded by three genes, and differential splicing leads to 10 to 12 isoforms, two antibodies were used to detect the predominant types of total JNK1 and JNK2 (12, 41). Anisomycin, a protein synthesis inhibitor and a known inducer of the JNK stress response, was added briefly before cell lysates were collected to stimulate the JNK pathway in positive-control cultures of HFFs (42). Again, lysates of mock-infected or VZV-infected cells were collected after 3 days. The amount of protein in each sample was adjusted so that equal amounts

were compared, as seen by the similar levels of total MKK4, MKK7, JNK, c-Jun, and β-actin (Fig. 1). Although these proteins were present in roughly equivalent amounts, their phosphorylation increased in both the anisomycin-treated control and VZV-infected cells. Anisomycin caused extensive phosphorylation of both forms of MKK4, while VZV infection resulted in heavy phosphorylation of only the slower-migrating form. VZV infection led to heavy phosphorylation of the faster-migrating form of phospho-MKK7, whereas treatment with anisomycin led to moderate phosphorylation of both forms of MKK7. The differences in phosphorylation patterns suggest that the JNK pathway responds differently to the VZV and anisomycin stimuli. The substantial increase in phospho-MKK7 levels is noteworthy and suggests that MKK7 is the main activator of JNK in VZV-infected cells. Differences in the phosphorylation patterns were also observed for JNK and c-Jun. Immunoblotting confirmed that VZV infection led to greater phosphorylation of JNK than anisomycin treatment. The abundance of phospho-JNK in the VZV-infected sample
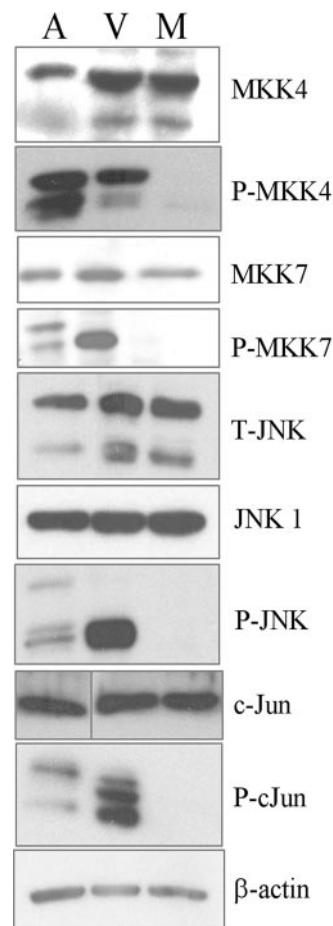

FIG. 1. The JNK pathway is induced by VZV. HFF cells were either mock infected or infected with VZV for 3 to 4 days. Cells treated with anisomycin (250 ng/ml for 30 to 40 min) were used as a positive control for induction of the JNK pathway. Lysates were then collected and used for immunoblotting. The results are representative of more than three experiments. β-Actin levels were used as a loading control. M, mock infected; V, VZV infected; A, anisomycin treated; P, phospho; T, total.
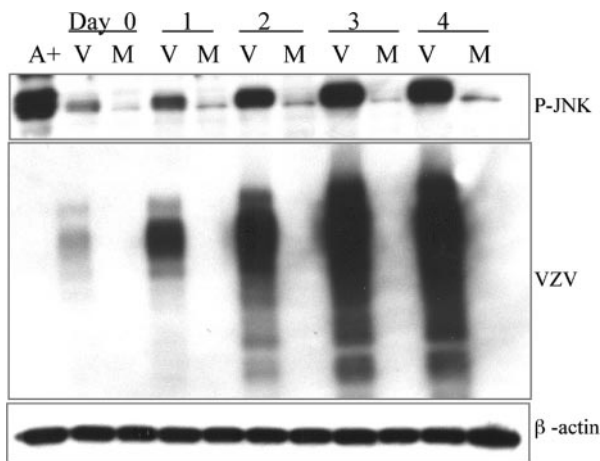
FIG. 2. Time course of JNK activation. Lysates of VZV- and mock-infected cells were collected at 2 h postinfection (day zero), day 1, day 2, day 3, and day 4 and were analyzed by immunoblotting. Blots were probed for phospho-JNK (P-JNK) and VZV antigen. Anisomycin-treated cells were used as a positive control. β-Actin levels were used as a loading control. M, mock infected; V, VZV infected; A+, aniso-mycin-treated positive control.

obscured a doublet of approximately 46 kDa (data not shown) that was visible in the anisomycin-treated sample, where less was present. These isoforms are likely splice variants of JNK1 and JNK2. Immunoblotting of phospho-c-Jun showed that VZV infection led to increased phosphorylation of several forms of c-Jun and JunD, which appeared as a cluster of bands at approximately 37 kDa. Importantly, no phosphorylated forms of the JNK pathway proteins were detected in mock-infected cultures, indicating that the experimental conditions did not inadvertently trigger a stress response. These results confirm and expand the observations made with the Kinexus arrays and indicate that the JNK pathway is conspicuously phosphorylated in VZV-infected HFFs in a manner different from that of the standard activator, anisomycin.

To determine the kinetics of JNK phosphorylation caused by the virus, HFF cultures were either inoculated with VZV-infected HFFs or mock infected with the same number of HFFs in suspension. This procedure results in approximately 1 cell in 100 becoming infected, or a multiplicity of infection (MOI) of 0.01. A higher MOI and cell-free virus cannot be obtained with VZV, thus precluding synchronous infections and analysis of early time points. After a 2-h adsorption (day 0), lysates of VZV- and mock-infected cells were collected daily and analyzed by immunoblotting for VZV glycoproteins, to monitor the progression of virus spread, and for phospho-JNK. Phospho-JNK levels increased over 4 days in parallel with the accumulation of VZV antigen, suggesting a correlation between virus replication and JNK phosphorylation (Fig. 2). At day 0, the level of phospho-JNK was greater in VZV-infected cells than in mock-infected controls, since the infection was initiated with a cell-associated virus that would already contain elevated phospho-JNK levels. The mock-infected cells maintained a consistently low level of phospho-JNK throughout the experiment. Thus, phospho-JNK was sustained in VZV-infected cultures and increased in direct proportion to virus spread.

The JNK inhibitor SP600125 prevents VZV replication. The extensive phosphorylation of JNK could have resulted from several possible effects: (i) incidental activation of the pathway by virus infection, (ii) a generic stress response, (iii) a specific cellular response to counteract the virus, such as apoptosis, or (iv) induction by the virus to favor its replication. To discern whether JNK phosphorylation was incidental, deleterious, or enhancing to VZV, the JNK inhibitor SP600125 was used to block the activity of this kinase. SP600125, an ATP analog, is a reversible, competitive JNK inhibitor that inserts into the ATP binding cleft (3, 27). Confluent HFFs were preincubated for 40 min with increasing amounts of SP600125 and were then infected with VZV. The inhibitor was refreshed every 24 h. After 48 h of infection, the monolayers were dispersed with trypsin to obtain a single-cell suspension, and the number of VZV-infected cells was determined by a plaque assay. SP600125 caused a dose-dependent reduction in VZV yield, with 50% inhibition of VZV replication (50% effective concentration) at approximately 8 μM (Fig. 3A). At a higher dose of 20 μM SP600125, immunofluorescence microscopy revealed that VZV was restricted to single cells or plaques consisting of only a few cells, which probably represent the inoculum or limited spread to adjacent cells (Fig. 3C). In contrast, large plaques formed in cultures treated with the diluent alone.

Examination of the treated monolayers by inverted phase-contrast microscopy did not show signs of toxicity at concentrations up to 20 μM, although adverse effects may not have been visible. To measure the cytotoxicity of SP600125 more accurately, a neutral red dye uptake assay was performed. Neutral red is absorbed by healthy, live cells and excluded by dying and dead cells, and it can be extracted for a quantitative measure of cell number and viability. Subconfluent monolayers of HFFs were treated either with diluent alone (DMSO) or with 5 to 40 μM SP600125 for 48 h (the drug was refreshed at 24 h). Compared to the rapid cell death observed with 35 nM staurosporine, an inducer of apoptosis, SP600125 did not cause a significant loss of cells at concentrations up to 40 μM (Fig. 3D). There was some decrease in cell number in all samples, including the untreated control, an indication that the cultures were densely packed. Since very little phosphorylated JNK was detected in confluent HFF cultures by immunoblotting, it is reasonable that a JNK inhibitor would have a minor impact on cell viability.

There was a possibility that intracellular or intranuclear JNK was not accessible to SP600125, so the phosphorylation of c-Jun was used as an indicator of inhibitor specificity; if SP600125 blocked the JNK ATP-binding site, then it could not phosphorylate c-Jun. JNK was induced in confluent monolayers by anisomycin treatment or VZV infection. Replicate samples were then treated with increasing amounts of SP600125. As expected, phosphorylation of c-Jun decreased in the presence of 9 μM SP600125 and was fully eliminated by 18 μM (Fig. 3B). Importantly, treatment with a dose as high as 70 μM did not affect the level of total c-Jun protein, VZV antigen, or β-actin, further evidence that the inhibitor was not acutely cytotoxic. Taken together, the results with SP600125 suggest that the induction of phosphorylated JNK is beneficial, even essential, for VZV replication and that it is not a spurious effect of virus infection or stress.
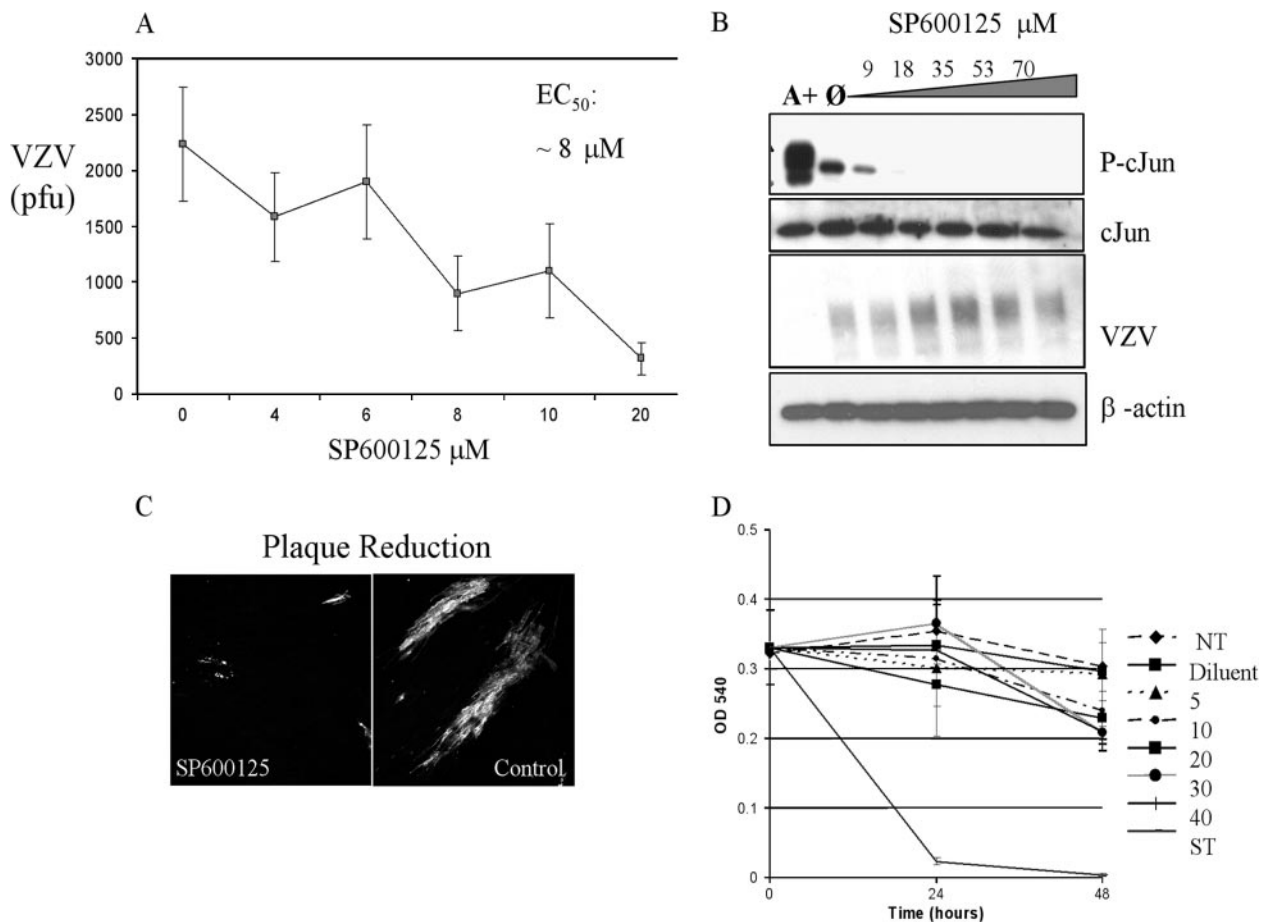
FIG. 3. Effects of SP600125 on VZV replication. (A) Dose dependence of SP600125. HFF cells were infected with VZV and treated either with increasing amounts of SP600126 (0 to 20 μM) or with diluent alone. The yield of VZV was determined by a plaque assay. (B) Specificity of SP600125. Lysates of VZV-infected cells, treated with increasing amounts of SP600126, were analyzed by immunoblotting and probed for phospho-c-Jun (P-cJun), c-Jun, and VZV antigen. A+, anisomycin-treated positive control; Ø, no inhibitor added. (C) Plaque reduction assay. Confluent HFF cells were either mock infected or VZV infected on glass slides for 48 h, with or without 20 μM SP600125. Control cells were treated with an equivalent amount of diluent (DMSO). Slides were analyzed by immunofluorescent confocal microscopy. (D) The cytotoxicity of SP600125 was determined by a neutral red uptake assay. NT, no treatment.

JNK activity in VZV-infected cells. The findings that JNK was highly phosphorylated in VZV-infected cells and that SP600125 treatment reduced c-Jun phosphorylation pointed toward the presence of enzymatically active JNK in these cells. However, it was possible that JNK activity was abnormal in VZV-infected cells. To address this question, kinase assays were performed to measure JNK activity. Cell lysates were prepared that had been either treated with anisomycin, infected with VZV for 3 days, or mock infected with an equal number of normal HFFs. c-Jun-GST immobilized on beads coated with glutathione was added to the cell lysates to pull down the JNK complex and provide an enzyme substrate. JNK activity, as shown by phosphorylation of the 37-kDa c-Jun-GST, was considerably greater in VZV-infected cells than in anisomycin-treated cells; in both, JNK activity was above the baseline activity levels observed in mock-infected cells (Fig. 4). Parallel kinase reactions were performed in the presence of 20 μM SP600125 in order to determine the specificity of the kinase-substrate interaction; it was possible that other kinases were pulled down and could have contributed to the

phosphorylation of c-Jun. Indeed, c-Jun phosphorylation was blocked in the presence of SP600125, indicating that JNK was the major kinase in the reaction. Immunoblotting confirmed that JNK protein was present in all samples but that only phospho-JNK was active. An important negative control was performed using glutathione beads to assess the level of background kinase activity that could have bound to the beads. The anisomycin-treated and mock-infected controls were free of kinase activity on glutathione beads, whereas the VZV-infected lysates produced several phosphoproteins in the 39- to 40-kDa range. These phosphoproteins were resistant to SP600125 treatment, and total JNK was not detected by immunoblot analysis of the proteins bound to glutathione beads, both indications that the background kinase activity was not due to JNK. One possible explanation is that VZV or cell kinases may have bound to the beads and phosphorylated other proteins in the complex. These results establish that the phospho-JNK detected in VZV infected cells by immunoblot is active and can serve as a marker for JNK activity.
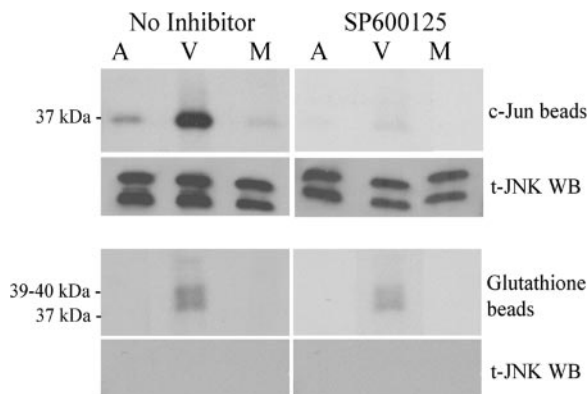
FIG. 4. JNK is more active in VZV-infected cells. Mock-treated, VZV-treated, and anisomycin-treated lysates were incubated with c-Jun beads (c-Jun–GST attached to glutathione beads) in order to pull down JNK. [γ-^{32}P]ATP was added, and phosphorylation of c-Jun was used as a measure of kinase activity. Shown is an autoradiograph of c-Jun phosphorylation. Mock-, VZV-, and anisomycin-treated lysates were also incubated with glutathione beads as a negative control (also shown as an autoradiograph). Kinase assays were performed either with or without SP600125 (20 μM). Western blotting (WB) was performed to determine the presence of JNK in the pulldowns. M, mock infected; V, VZV infected; A, anisomycin treated; t, total.

Activated JNK localizes to the nucleus in VZV-infected cells. The location of phosphorylated JNK within the cell determines its access to substrates and potential interacting proteins, both viral and cellular. Intracellular localization also points to possible functions of JNK in VZV-infected cells, such as activation of transcription factors in the nucleus or modification of cellular factors in the cytoplasm. To determine whether the JNK pathway was activated in all cells or only in VZV-infected cells, and to identify the subcellular compartment where activated JNK and c-Jun were located, confocal immunofluorescence microscopy was employed. Confluent HFFs were either infected with VZV or mock infected for 24 to 48 h on glass chamber slides and were then probed with rabbit antibodies to phospho-JNK or phospho-c-Jun and a panspecific human antiserum that detects VZV glycoproteins. It is known that activation of JNK is associated with its accumulation in the nucleus (6), so it was not surprising to find phosphorylated JNK in the nuclei of VZV-infected cells (Fig. 5A). Phospho-JNK was occasionally detected in the nuclei of cells outside VZV plaques, although most of the infected cells contained phospho-JNK in their nuclei. An expanded view of a single infected cell showed an interesting pattern of phospho-JNK in many small nuclear foci (Fig. 5B). The confinement of phospho-JNK to the VZV plaques indicated that JNK activation was not a paracrine or stress effect of VZV infection. Evidence of widespread JNK activation was observed in cells treated with anisomycin (Fig. 5C), while mock-infected cells showed basal levels of phospho-JNK that were barely detectable in the cytoplasm (Fig. 5D). A control for nonspecific antibody binding was performed using normal rabbit serum on VZV-infected HFFs, since this virus produces a gE-gI heterodimer that can function as an Fc receptor (45); the nonspecific rabbit serum and secondary antibodies did not bind to VZV plaques (Fig. 5E).

The pattern of phospho-c-Jun localization mirrored that of phospho-JNK. Phospho-c-Jun was detected in the nuclei of VZV-infected cells and rarely outside plaques (Fig. 5F). Translocation of c-Jun from the cytoplasm to the nucleus upon phosphorylation by JNK is the typical route of transcription factors, since they operate mainly in the nucleus. Anisomycin also caused phospho-c-Jun to accumulate in nuclei, and these activated cells were shrunken and appeared to be undergoing apoptosis (Fig. 5G). Mock-infected cells showed a basal level of phospho-c-Jun in the cytoplasm (Fig. 5H). Again, VZV plaques did not bind antibodies nonspecifically (Fig. 5I). Together these micrographs illustrated the pronounced activation of the JNK pathway in infected cells and showed movement of key factors into the nucleus, where they may have a role in VZV replication events such as transcriptional activation and protein phosphorylation.

Tracking the induction of JNK by confocal microscopy provided an approach to studying the kinetics of JNK activation that did not depend on a high MOI. Analysis of phospho-JNK at the edges of plaques, where infection was most recent, and the use of the viral DNA polymerase inhibitor phosphono-acetic acid (PAA) to block late gene expression, enabled us to address the question of when during VZV replication JNK was activated. Confluent cells were either infected with VZV or mock infected for 24 h on glass chamber slides, treated with PAA or diluent, and then probed with antibodies to phospho-JNK and the VZV major immediate-early protein encoded by ORF62 (IE62). IE62 follows a predictable course of strict nuclear localization at early times; then, at later times, it is phosphorylated by the ORF66 kinase and shuttles between the nucleus and the cytoplasm (38, 40). By using this pattern as a guide, cells were identified where phospho-JNK colocalized with IE62 exclusively in the nucleus, indicating an early activation (Fig. 6A). At later times, when IE62 was abundant in all cell compartments, most phospho-JNK remained in the nuclei and only a small fraction was observed colocalizing with IE62 in the cytoplasm. In the absence of PAA, 87% of VZV-infected cells were in late stages of infection (cytoplasmic IE62) and 12% were in early stages (strict nuclear localization). All late infected cells were positive for nuclear phospho-JNK, while 86% of early infected cells were positive for nuclear phospho-JNK. In the presence of PAA, IE62 was restricted to nuclei and colocalized extensively with phospho-JNK (Fig. 6E). Of the VZV-infected cells, 80% were in early infection, 20% were in late infection, and all had nuclear phospho-JNK. A portion of phospho-JNK was also in the cytoplasm under these conditions. It should be noted that under both experimental conditions (with or without PAA), cells were found that had nuclear phospho-JNK but were devoid of IE62. These bystander cells were adjacent to plaques and clustered around infected cells. They probably represent earlier stages of infection when viral antigen is undetectable. Thus, these experiments show that the activation of JNK occurred early during VZV replication.

The localization of phospho-JNK in the cytoplasm was also observed using a polyclonal serum that binds many VZV proteins, including glycoproteins. These single infected cells were scattered throughout the HFF monolayer and often had long membrane extensions that stained brightly for VZV (Fig. 6I to K) and for phospho-JNK. Where an extension contacted an adjacent cell, phospho-JNK appeared in the nucleus of a cell that was negative for VZV antigen (Fig. 6K). Numerous ex-
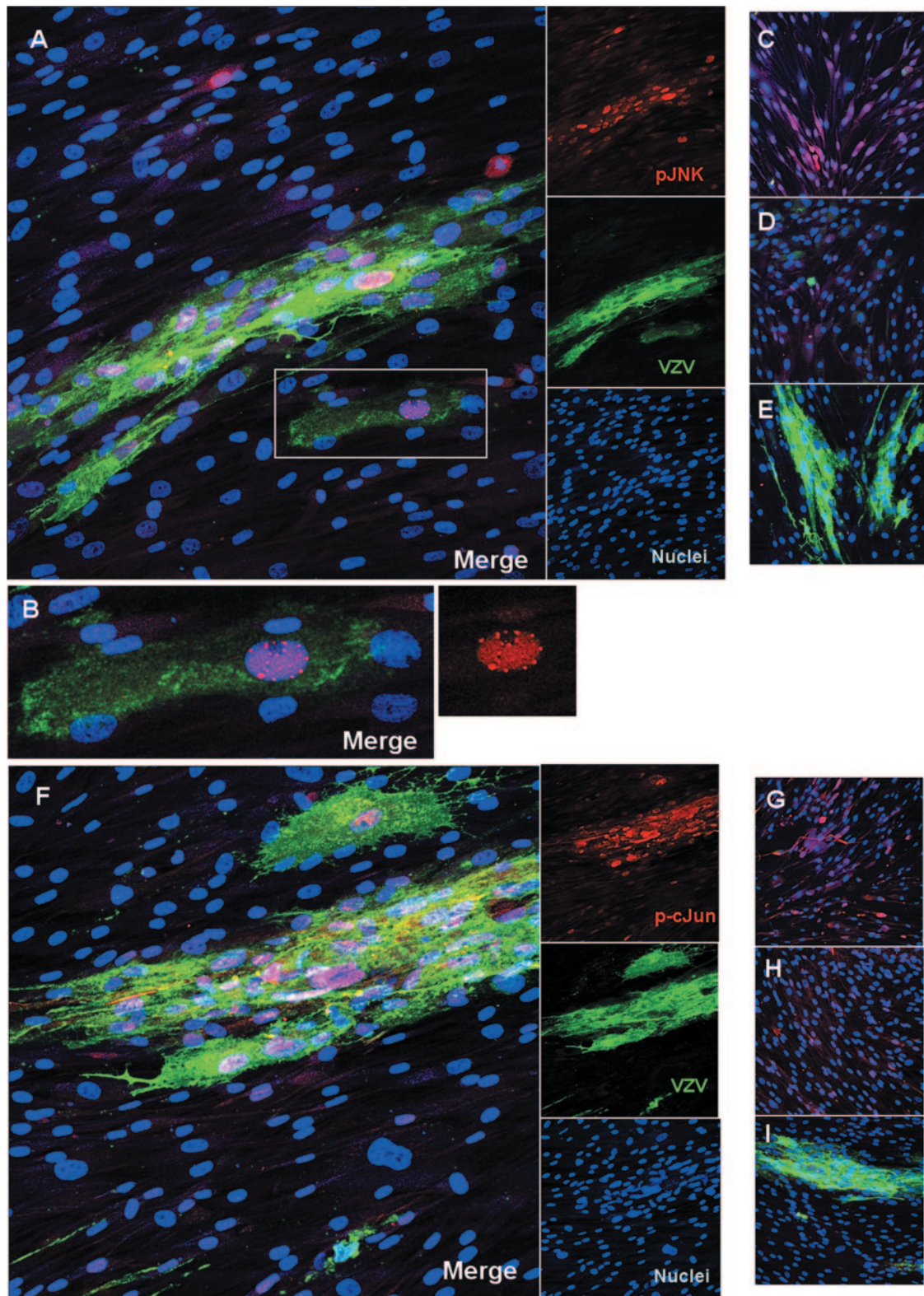
FIG. 5. Phospho-JNK and phospho-c-Jun accumulate in the nuclei of VZV-infected cells. (A through E) Localization of phospho-JNK. Anisomycin-treated cells were used as a positive control. Confluent cells were either mock infected or VZV infected for 24 h on glass slides. Slides were fixed and probed for phospho-JNK and VZV glycoproteins. Proteins were visualized using immunofluorescent confocal microscopy. (A) Phospho-JNK localizes to the nuclei of VZV-infected cells. (B) Enlargement of boxed area in panel A. The smaller panel on the right shows an enlargement of the red channel alone. (C) Anisomycin-treated cells, used as a positive control. (D) Mock-treated cells. (E) Antibody control with VZV-infected cells. (F through I) Localization of phospho-c-Jun. (F) Phospho-c-Jun localizes to the nuclei of VZV-infected cells. (G) Anisomycin-treated cells, used as a positive control. (H) Mock-treated cells. (I) Antibody control with VZV-infected cells. Red, phospho-JNK or phospho-c-Jun; green, VZV glycoproteins; blue, nuclei. Magnification, ×200.
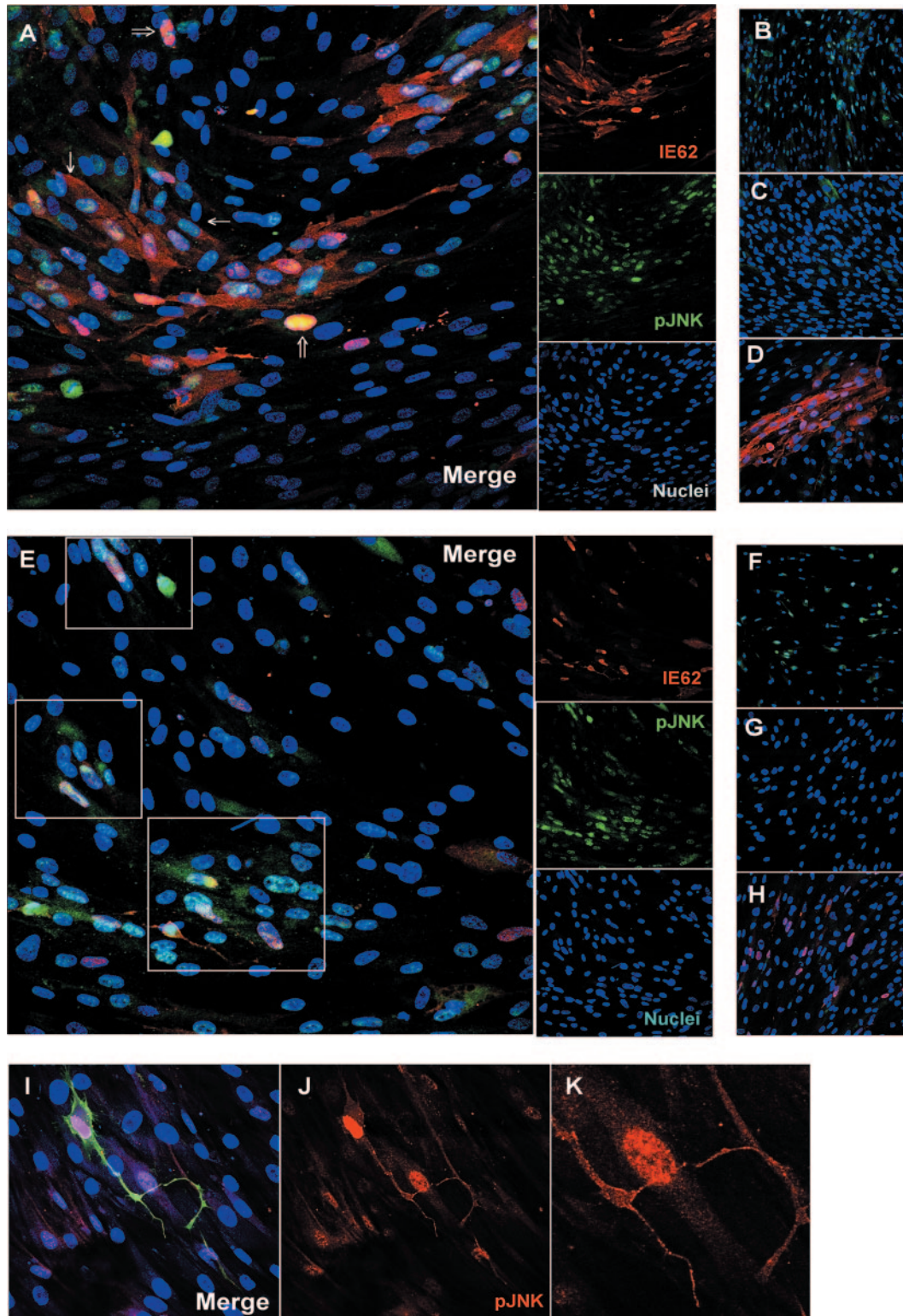
FIG. 6. Phospho-JNK accumulates in the nuclei of infected cells at early times. Confluent cells were either mock infected or VZV infected for 24 h on glass slides in the absence of PAA (A to D) or with PAA (E to K). Anisomycin-treated cells were used as a positive control. Slides were fixed and probed for phospho-JNK and IE62. Proteins were visualized using immunofluorescent confocal microscopy. (A) VZV-infected cells in the absence of PAA. Thin arrows indicate late infected cells, with cytoplasmic IE62 and nuclear phospho-JNK. Thick arrows indicate early infected cells, where IE62 is entirely nuclear and phospho-JNK is present in the nucleus. (B) Anisomycin-treated cells. (C) Mock-treated cells. (D) Antibody control with VZV-infected cells. (E) VZV-infected cells in the presence of PAA. Areas of colocalization between phospho-JNK and nuclear IE62 are boxed. (F) Anisomycin-treated cells. (G) Mock-treated cells. (H) Antibody control with VZV-infected cells. For panels A through H, IE62 stained red, phospho-JNK stained green, and nuclei stained blue. (I) Confluent cells were infected with VZV for 24 h on glass slides in the presence of PAA. Slides were fixed and probed for phospho-JNK (red), VZV glycoproteins (green), and nuclei (blue). (J) Red channel. Red, phospho-JNK. (K) Enlargement of an area of panel J. Magnification, ×200 (A to H); magnification, ×400 (I to K).
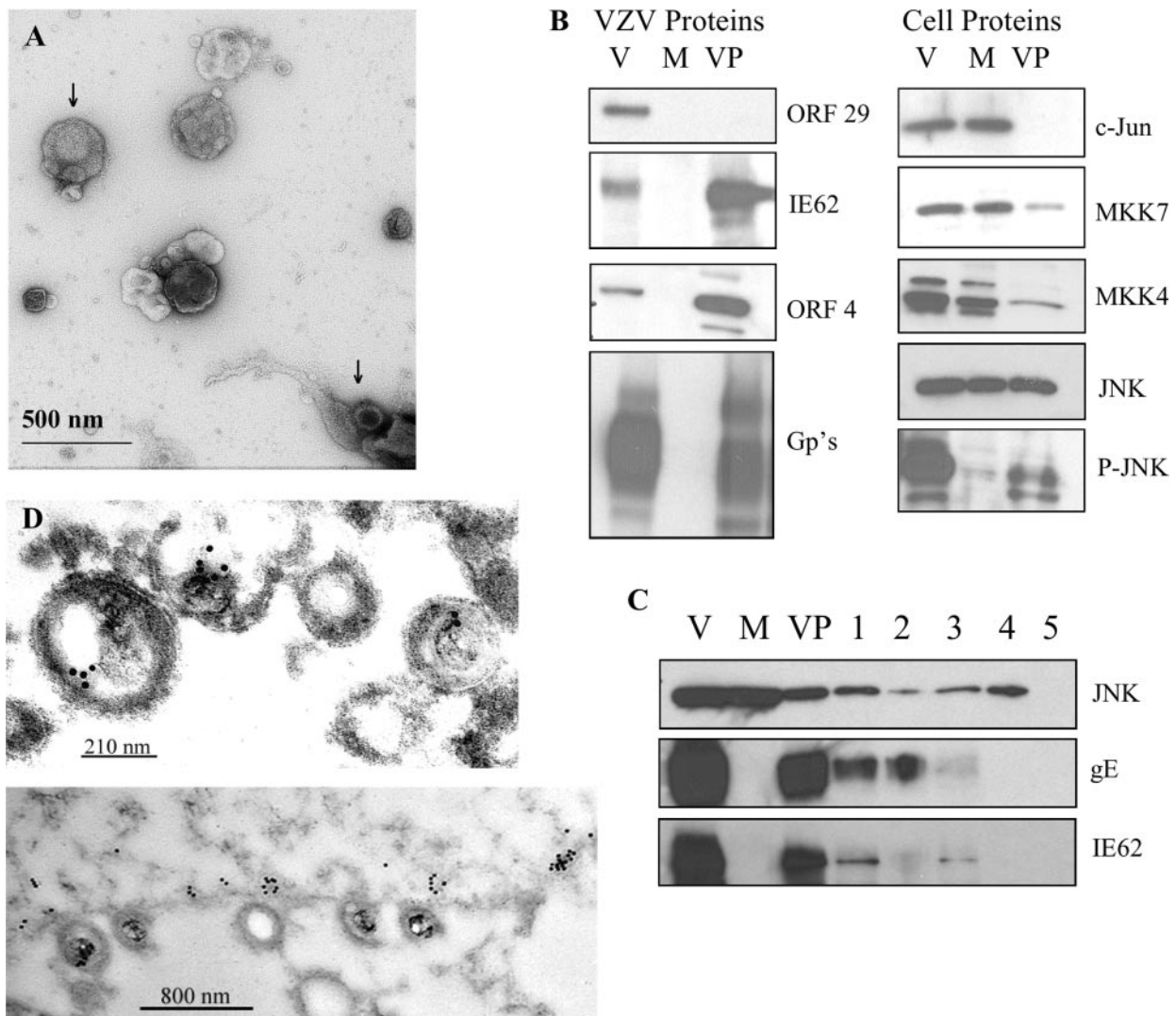
FIG. 7. JNK is incorporated into VZV virions. (A) Negative stain of purified VZV virions. VZV particles were negatively stained with 1% uranyl acetate and viewed by TEM (magnification, ×49,000). The top arrow indicates an intact virion with a visible nucleocapsid. The bottom arrow indicates a disrupted virion with the nucleocapsid and tegument spilling out of the envelope. (B) Purified virions were analyzed by immunoblotting and probed with antibodies to the proteins indicated. V, VZV-infected cell lysate; M, mock-infected cell lysate; VP, purified virion particles. (C) Virion detergent and protease treatments. Purified virions were treated with 1% Triton X-100 for 30 min and separated into two fractions: the pelleted virus particles (lane 1) and the supernatant (lane 2). Purified virions were also treated with trypsin alone for 15 min (lane 3) and with trypsin and 1% Triton X-100 for 5 (lane 4) or 15 (lane 5) min. Treated virions were analyzed by immunoblotting and probed with appropriate antibodies. VP, untreated virus particles. (D) Immunoelectron microscopy. Heavily infected cells were sectioned, probed with a polyclonal anti-JNK antibody and a secondary antibody conjugated to 10-nm-diameter gold beads, and viewed by TEM. Magnification: ×40,000 for the top panel and ×10,000 for the bottom panel.

amples of this were observed (images not shown). In the presence of PAA, only the cell-associated inoculum would express preexisting late proteins, such as glycoproteins, that are mainly recognized by this antiserum. Since late gene expression is blocked by PAA, this suggests that contact or infection by the inoculum cell can activate JNK early during VZV replication.

JNK is incorporated into VZV virions. The observation of phospho-JNK in the cytoplasm of infected cells led to the question of whether it was associated with VZV particles, which assemble in the cytoplasm and egress along membrane extensions and tracts (also known as viral highways) (25, 65). VZV assembly is characterized by degradation of the virions in acidic vacuoles (21), so virus was grown in a MeWo mutant cell line, MPR-KD, in which the mannose-6-phosphate receptor, involved in trafficking to late endosomes and lysosomes, is knocked down (7). Virions were isolated from culture supernatants and from infected cells disrupted by gentle Dounce homogenization; then they were purified through Ficoll. Negative staining and transmission electron microscopy confirmed the integrity and purity of the virion preparation (Fig. 7A). Intact virion particles with visible nucleocapsids were present throughout the preparation. Some broken and disrupted virions, where the nucleocapsid and tegument spilled out of the envelope, were also seen. No intact cells or nuclei were found.

Glycoproteins and tegument proteins (ORF4, IE62) were detected by immunoblotting in an infected-cell lysate and in the virion particles (36, 37, 39), while the single-stranded DNA-binding protein ORF29 was found only in the cell lysate (Fig. 7B). This was confirmation that the virion preparation did not contain contaminating nuclei or viral DNA, since the packaged genomes are not associated with ORF29 protein (35, 36). No viral proteins were detected in the mock-infected MeWo cell lysate. As expected, JNK was detected in both the VZV-infected and mock-infected lysates; surprisingly, it was detected in the virions as well. Similarly, phospho-JNK was detected in the VZV-infected cell lysates and in the virions. This indicated that active JNK was associated with the VZV particles and could be transferred with the virus to new cells. Other members of the JNK pathway were also examined by immunoblotting. The transcription factor c-Jun was absent from virions, although MKK7 and MKK4 were present in small amounts.

The presence of JNK in the virion was further confirmed by detergent and protease treatments. Purified virions were treated with 1% Triton X-100 and subjected to high-speed centrifugation, thus releasing envelope proteins into the supernatant. The pelleted virus particles and the supernatant were analyzed by immunoblotting (Fig. 7C, lanes 1 and 2). JNK associated primarily with the pelleted virus particles, although some was solubilized. In contrast, the tegument protein IE62 associated entirely with the pelleted virus particles, while about half of the glycoprotein E, a major constituent of the viral envelope, was solubilized. This indicates that JNK and IE62 are located internally within the virion and that the membrane containing gE remained associated with virus particles. When the purified virions were treated with trypsin alone (Fig. 7C, lane 3), glycoprotein E was entirely digested, while JNK and IE62 remained in the virion pellet. A small portion of JNK and IE62 was digested by trypsin, since some of the virion envelopes were torn (Fig. 7A). When virions were subjected to combined trypsin and 1% Triton X-100 treatment (Fig. 7C, lanes 4 and 5), JNK persisted within the virion pellet for 5 min and was completely digested after 15 min. IE62 and gE were undetectable after 5 min. This suggests that JNK is perhaps more tightly associated with the virion than IE62. These results indicate that the viral envelope protected JNK from trypsin digestion; thus, JNK is located inside virions, specifically within the tegument layer.

The possibility remained that the presence of JNK in VZV virion preparations was due to contaminating virion-like structures that had biophysical properties similar to those of virions. In order to validate the novel finding that JNK associated with the VZV tegument, immunogold transmission electron microscopy was performed (Fig. 7D). Heavily infected cells were analyzed by immuno-TEM with a polyclonal rabbit antibody to JNK and a secondary antibody conjugated to 10-nm-diameter gold beads. Gold beads were broadly distributed in the cytoplasm of infected cells, and small clusters were found associated with virions that aligned on the extracellular side of the plasma membrane. Gold particles were specifically bound to the tegument layer of the virion on the outside face of the nucleocapsid. Interestingly, small patches of gold beads accumulated along the intracellular side of the plasma membrane, often directly under virions that studded the membrane. The negative-control sections treated with nonspecific rabbit immu-noglobulin G were free of gold particles (data not shown). Additionally, positive-control sections were treated with a polyclonal rabbit antibody to the viral tegument protein IE62, and numerous gold particles associated with virions (data not shown), which has been reported previously (37).

DISCUSSION

This study demonstrates that VZV manipulates the JNK pathway and depends on its activity for replication. Furthermore, phospho-JNK is assembled into VZV particles and may have important functions in newly infected cells. The findings raise a number of issues about the interaction of VZV with cell signaling networks: the pattern of JNK pathway activation, the different effects of VZV in other cell types, and possible functions of activated JNK in infected cells. The major question, and the one most difficult to answer, is the mechanism of JNK activation by VZV. Related to this is the unknown antiviral mechanism of the JNK inhibitor SP600125. Despite our incomplete understanding of the molecular role of JNK in VZV infection, the results presented here show that inhibition of JNK is a plausible antiviral strategy against VZV.

The JNK pathway was activated at three levels—the MAP2K level (MKK4, MKK7), the MAPK level (JNK), and the substrate level (c-Jun, JunD)—as indicated by increased phosphorylation of these proteins and increased JNK activity. SP600125 inhibited c-Jun phosphorylation in vitro and in VZV cultures, which is evidence that no cell or viral kinases other than JNK were involved. However, VZV-infected cells had a kinase activity associated with glutathione beads that was resistant to SP600125, indicating that this kinase activity was not due to JNK. VZV encodes two viral kinases, ORF66 and ORF47, with predicted sizes of 46 and 54 kDa, respectively (34). These are both larger than the 40-kDa phosphoprotein that appeared in the control kinase assays, so autophosphorylation is not a likely possibility. VZV or cell kinases may have bound to the beads and phosphorylated other proteins in the complex; further analysis by immunoblotting would be required to confirm this hypothesis.

The antiviral effects of SP600125 indicate how important the JNK pathway is to VZV and promote the idea that JNK is a potential therapeutic target. Targeting the JNK pathway for therapeutic benefit is a goal that both researchers and drug companies are pursuing. The JNK pathway is considered a target for the treatment of cancer and diseases caused by inflammation and neurodegeneration (12, 48). Several derivatives of SP600125 have been developed and are progressing in clinical trials for these applications (48). Thus, there is potential for treating viral infections, including VZV, with JNK inhibitors. Inhibition of the JNK pathway is known to interfere with the functions of other viruses. SP600125 inhibits the activation of JNK by the hepatitis C virus protein NS3, which contributes to hepatitis C virus-related hepatocarcinogenesis (26). For HSV-1, expression of the scaffold protein JIP-1, which effectively inhibits JNK translocation to the nucleus, decreases the HSV-1 yield by 70% (49).

Observing where activated JNK was located in VZV-infected cells uncovered its predicted migration to the nucleus, its induction early in virus replication, and an unexpected appearance in cell extensions and virions. JNK is located in both

the cytoplasm and nuclei of quiescent cells; stimulation by UV irradiation is known to cause accumulation of phospho-JNK-1 in the nucleus (6). Finding phospho-JNK in discrete nuclear foci (speckles) within VZV-infected cells pointed to areas with concentrated JNK activity, perhaps where viral transcription was occurring. There is evidence that signaling kinases may form integral components of transcription complexes, thus influencing gene expression (16). Evidence for the accumulation of JNK in the nucleus has also been shown for HSV-1 (49). Like JNK, c-Jun migrated to the nuclei of infected cells. These translocations were specifically induced by VZV, since activated JNK and c-Jun were at basal levels in the cytoplasm of uninfected cells at the plaque borders. This is evidence that activation of the JNK pathway was not a paracrine or stress-induced effect. Activated JNK was also found in the nuclei of infected cells that expressed nuclear IE62 (early-stage infection) and that were treated with PAA to block late gene expression, supporting the contention that JNK is activated early. Moreover, phospho-JNK was present in nuclei adjacent to infected cells that did not yet show detectable levels of IE62, which could occur by way of signaling events associated with virus attachment or penetration. Alternatively, activated JNK protein could be transferred directly. Either possibility is supported by the observation that phospho-JNK was located in far-reaching cytoplasmic extensions that could fuse or deliver virions to new cells. The unforeseen association of activated JNK with VZV virions, the first report for a virus, strengthens the potential for direct transfer of this protein to new cells. Although the kinetics and mechanism of JNK activation by VZV are unclear, the events surrounding the initial activation of the JNK pathway in VZV-infected cells are of great interest and are being pursued.

Several possibilities for VZV activation of the JNK pathway are being considered and follow from the finding that MKK4 and MKK7 were heavily phosphorylated. One is that signals from membrane receptors resulted in phosphorylation of these MAP2Ks, and another is that VZV infection activated the pathway at an intermediate level. Typically, MKK7 protein kinase is activated by cytokines (tumor necrosis factor, interleukin-1), and MKK4 is activated by environmental stresses (12). These ligands engage specific receptors that activate any number of MAP3Ks, which then activate MKK4 and MKK7. Identification of the MAP3Ks involved is severely hindered by the facts that (i) the VZV surface receptor is unknown, (ii) linking specific stimuli (such as UV irradiation) to particular MAP3Ks is very difficult, and (iii) the MAP3Ks involved in JNK activation vary by cell type. Furthermore, the physiological relevance of MAP3Ks is uncertain, and many promiscuously activate more than one pathway (12, 31). VZV infection could also cause MKK4, MKK7, or JNK activation by a viral or cellular kinase other than the MAP3Ks. Finally, VZV could cause the sustained activation of JNK by the modulation of phosphatases. The MAPKs, including JNK, are inactivated by a group of 10 MAPK phosphatases (31, 69). The balance between activating MAP2Ks, such as MKK4 and MKK7, and MAPK phosphatases determines the duration and magnitude of JNK activation. VZV disruption of this balance is manifested by the sustained and increasing JNK activation seen over 4 days of virus replication. VZV activation of the JNK pathway appears to differ from normal cell processes, since

infection produced a pattern distinctly altered from that of anisomycin. Only certain isoforms of these kinases were preferentially phosphorylated in VZV-infected cells, suggesting that VZV signaling through the JNK pathway is precisely regulated. The differential phosphorylation of JNK by MKK4 and MKK7 may generate a cellular response that is unique to VZV and optimal for its replication.

There is some evidence from other reports that VZV and its close relative HSV-1 interact with the JNK pathway after entry. The HSV-1 immediate-early protein ICP27 was found to be solely necessary for the activation of JNK in the context of infection (24). In HSV-1, ectopically overexpressed ICP0 has also been reported to activate the JNK pathway (14). Similarly, the VZV homolog of ICP0, ORF61, activates JNK when ORF61 is expressed ectopically (61). However, the activation of JNK by ORF61 is linked with a twofold reduction in VZV yield that could be reversed by treating the cultures with JNK inhibitor 1, a recombinant fusion of the JNK scaffold protein (islet-brain 1 and 2 proteins) and a membrane permeable peptide (HIV-Tat) (4, 62). That report contradicts the antiviral effects of SP600125 presented here but confirms the activation of JNK in VZV-infected cells. Differences in the cell types and inhibitors used could account for the discrepancy. Primary cells were used in this study, while melanoma cells (MeWo) were used elsewhere. Melanoma cells are a tumor cell line and thus may have oncogenic mutations that alter signaling networks and sensitivity to inhibitors. The mechanism of action of SP600125, an ATP analog, is fundamentally different from that of JNK inhibitor 1, a JNK-binding protein. Ultimately, the interaction between VZV and the JNK pathway is likely to have redundant mechanisms, as is true of HSV-1, and to be specific for each cell type studied.

Activation of the JNK pathway is common to herpesviruses, although the purpose in virus replication is not fully understood (17, 23, 33, 49, 74). The advantages of JNK activation for herpesviruses relate to its spectrum of functions in the cell; JNK is involved in the regulation of gene expression, apoptosis, cell migration, and responses to environmental stresses. The recruitment of phospho-JNK to the nucleus points to a possible role of JNK in transcription. JNK substrates include the transcription factors c-Jun, ATF-2, and Elk-1 (41); c-Jun and ATF-2 are needed for VZV replication (64); therefore, VZV may activate JNK to increase viral gene expression. The JNK pathway has also been implicated in both apoptosis and cell survival, depending on the cellular context (12, 30). VZV induces apoptosis in certain cell types, such as HFFs (28), but apoptosis was rare in this study (authors' observations), and no significant poly(ADP-ribose) polymerase cleavage was detected in VZV-infected MeWo cells (62). Additionally, treatment with anisomycin, a known inducer of apoptosis (67), showed a pattern of activation distinct from that of VZV infection. Thus, JNK activation seems unlikely to induce apoptosis in VZV-infected cells. Also, the JNK pathway is linked to cell migration (31, 72), and the movement of keratinocytes is impaired when they are exposed to SP600125 (29). The pseudorabies virus US3 kinase has been shown to cause dramatic alterations in the cytoskeleton, resulting in the formation of long cell projections that are associated with enhanced spread of the virus (19). Interestingly, VZV-induced cell extensions also contained phospho-JNK, and it would be interesting to

determine whether viral kinases were also involved. Therefore, it is conceivable that JNK would be activated to facilitate viral movement within the cell. Lastly, environmental stresses activate the JNK pathway, which may actually enhance virus replication. Recently it was reported that the infectivity of HSV-1 ICP0 mutants increased after the cells were stressed by heat shock and UVC irradiation (5). It is intriguing to speculate that these stresses activated the JNK pathway. Overall, JNK activation has various functions that may favor herpesviruses or that are even essential for replication.

Although the purpose of JNK activation for VZV replication remains to be studied, it is clear that the JNK pathway is crucial for many viruses. It is possible that upregulation of a cellular pathway determines, in part, the susceptibility of a cell to infection. For example, the Akt signaling pathway was recently found to be a key determinant for the permissiveness of human cancer cells to myxoma virus (70). Nonpermissive tumor cells supported myxoma virus replication after expression of active Akt. Conversely, permissive cancer cells were made nonpermissive by blocking Akt activation with a dominant-negative inhibitor. Therefore, cells lacking JNK might not be susceptible to VZV infection. Following this reasoning, it would be interesting to determine whether cells lacking JNK are permissive for VZV. In conclusion, the interaction of VZV with the JNK pathway is a clear example of viral coevolution with cellular signaling networks and underscores the dependence of viruses on their hosts. The idea of using host factors, as opposed to viral proteins, as drug targets opens up new avenues for the generation of new antiviral drugs and should be considered (10, 51).

REFERENCES

1. **Arvin, A.** 1996. Varicella-zoster virus, p. 2547–2585. *In* B. N. Fields, D. M. Knipe, and P. M. Howley (ed.), Fields virology, 3rd ed. Lippincott-Raven, Philadelphia, Pa.
2. **Babich, H., A. Sedletcaia, and B. Kenigsberg.** 2002. In vitro cytotoxicity of protocatechuic acid to cultured human cells from oral tissue: involvement in oxidative stress. Pharmacol. Toxicol. **91:**245–253.
3. **Bennett, B. L., D. T. Sasaki, B. W. Murray, E. C. O'Leary, S. T. Sakata, W. Xu, J. C. Leisten, A. Motiwala, S. Pierce, Y. Satoh, S. S. Bhagwat, A. M. Manning, and D. W. Anderson.** 2001. SP600125, an anthrapyrazolone inhibitor of Jun N-terminal kinase. Proc. Natl. Acad. Sci. USA **98:**13681–13686.
4. **Bonny, C., A. Oberson, S. Negri, C. Sauser, and D. F. Schorderet.** 2001. Cell-permeable peptide inhibitors of JNK: novel blockers of B-cell death. Diabetes **50:**77–82.
5. **Bringhurst, R. M., and P. A. Schaffer.** 2006. Cellular stress rather than stage of the cell cycle enhances the replication and plating efficiencies of herpes simplex virus type 1 ICP0⁻ viruses. J. Virol. **80:**4528–4537.
6. **Cavigelli, M., F. Dolfi, F.-X. Claret, and M. Karin.** 1995. Induction of c-fos expression through JNK-mediated TCF/Elk-1 phosphorylation. EMBO J. **14:**5957–5964.
7. **Chen, J. J., Z. Zhu, A. A. Gershon, and M. D. Gershon.** 2004. Mannose 6-phosphate receptor dependence of varicella zoster virus infection in vitro and in the epidermis during varicella and zoster. Cell **119:**915–926.
8. **Chen, S.-Y., J. Lu, Y.-C. Shih, and C.-H. Tsai.** 2002. Epstein-Barr virus latent membrane protein 2A regulates c-Jun protein through extracellular signal-regulated kinase. J. Virol. **76:**9556–9561.
9. **Chen, Z., T. B. Gibson, F. Robinson, L. Silvestro, G. Pearson, B. Xu, A. Wright, C. Vanderbilt, and M. H. Cobb.** 2001. MAP kinases. Chem. Rev. **101:**2449–2476.
10. **Coen, D. M., and P. A. Schaffer.** 2003. Antiherpesvirus drugs: a promising spectrum of new targets and drug targets. Nat. Rev. Drug Discov. **2:**278–288.
11. **Damania, B., J.-K. Choi, and J. U. Jung.** 2000. Signaling activities of gammaherpesvirus membrane proteins. J. Virol. **74:**1593–1601.
12. **Davis, R. J.** 2000. Signal transduction by the JNK group of MAP kinases. Cell **103:**239–252.
13. **Derijard, B., M. Hibi, I.-H. Wu, T. Barrett, B. Su, T. Deng, M. Karin, and R. J. Davis.** 1994. JNK 1: a protein kinase stimulated by UV light and Ha-Ras that binds and phosphorylates the c-Jun activation domain. Cell **76:**1025–1037.
14. **Diao, L., B. Zhang, C. Xuan, S. Sun, K. Yang, Y. Tang, W. Qiao, Q. Chen, Y. Geng, and C. Wang.** 2005. Activation of c-Jun N-terminal kinase (JNK) pathway by HSV-1 immediate early protein ICP0. Exp. Cell Res. **308:**196–210.
15. **Dykstra, M. J., and L. E. Reuss.** 2003. Biological electron microscopy: theory, techniques, and troubleshooting, 2nd ed. Kluwer Academic/Plenum Publishers, New York, NY.
16. **Edmunds, J. W., and L. C. Mahadevan.** 2006. Protein kinases seek close encounters with active genes. Science **313:**449–451.
17. **Eliopoulos, A. G., and L. S. Young.** 1998. Activation of the c-Jun N-terminal kinase (JNK) pathway by the Epstein-Barr virus-encoded latent membrane protein 1 (LMP 1). Oncogene **16:**1731–1742.
18. **Evers, D. L., X. Wang, and E.-S. Huang.** 2004. Cellular stress and signal transduction responses to human cytomegalovirus infection. Microbes Infect. **6:**1084–1093.
19. **Favoreel, H. W., G. Van Minnebrugen, D. Adriaensen, and H. J. Nauwynck.** 2005. Cytoskeletal rearrangements and cell extensions induced by the US3 kinase of an alphaherpesvirus are associated with enhanced spread. Proc. Natl. Acad. Sci. USA **102:**8990–8995.
20. **Galdiero, S., M. Vitiello, M. D'Isanto, E. Di Niola, L. Peluso, K. Raieta, C. Pedone, M. Galdiero, and E. Benedetti.** 2004. Induction of signaling pathways by herpes simplex virus type 1 through glycoprotein H peptides. Biopolymers **76:**494–502.
21. **Gershon, A. A., D. L. Sherman, Z. Zhu, C. A. Gabel, R. T. Ambron, and M. D. Gershon.** 1994. Intracellular transport of newly synthesized varicella-zoster virus: final envelopment in the *trans*-Golgi network. J. Virol. **68:**6372–6390.
22. **Greber, U. F.** 2002. Signalling in viral entry. Cell. Mol. Life Sci. **59:**608–626.
23. **Hamza, S. M., R. A. Reyes, Y. Izumiya, R. Wisdom, H.-J. Kung, and P. A. Luciw.** 2004. ORF36 protein kinase of Kaposi's sarcoma herpesvirus (KSHV) activates the c-Jun N-terminal kinase (JNK) signaling pathway. J. Biol. Chem. **279:**38325–38330.
24. **Hargett, D., T. Mclean, and S. L. Bachenheimer.** 2005. Herpes simplex virus ICP27 activation of stress kinases JNK and p38. J. Virol. **79:**8348–8360.
25. **Harson, R., and C. Grose.** 1995. Egress of varicella-zoster virus from the melanoma cell: a tropism for the melanocyte. J. Virol. **69:**4994–5010.
26. **Hassan, M., H. Ghozlan, and O. Abdel-Kader.** 2005. Activation of c-Jun NH₂-terminal kinase (JNK) signaling pathway is essential for the stimulation of hepatitis C virus (HCV) non-structural protein 3 (NS3)-mediated cell growth. Virology **333:**324–336.
27. **Heo, Y. S., S. K. Kim, C. I. Seo, Y. K. Kim, B. J. Sung, H. S. Lee, J. I. Lee, S. Y. Park, J. H. Kim, K. Y. Hwang, Y. L. Hyun, Y. H. Jeon, S. Ro, J. M. Cho, T. G. Lee, and C. H. Yang.** 2004. Structural basis for the selective inhibition of JNK1 by the scaffolding protein JIP1 and SP600125. EMBO J. **23:**2185–2195.
28. **Hood, C., A. L. Cunningham, B. Slobedman, R. A. Boadle, and A. Abendroth.** 2003. Varicella-zoster virus-infected human sensory neurons are resistant to apoptosis, yet protected against cell death: evidence for a cell-type-specific apoptotic response. J. Virol. **77:**12852–12864.
29. **Huang, C., Z. Rajfur, C. Borchers, M. D. Schaller, and K. Jacobson.** 2003. JNK phosphorylates paxillin and regulates cell migration. Nature **424:**219–223.
30. **Ip, T. Y., and R. J. Davis.** 1998. Signal transduction by the c-Jun N-terminal kinase (JNK)—from inflammation to development. Curr. Opin. Cell Biol. **10:**205–219.
31. **Karin, M., and E. Gallagher.** 2005. From JNK to pay dirt: JNK kinases, their biochemistry, physiology and clinical importance. IUBMB Life **57:**283–295.
32. **Karin, M., Z.-G. Liu, and E. Zandi.** 1997. AP-1 function and regulation. Curr. Opin. Cell Biol. **9:**240–246.
33. **Kieser, A., E. Kilger, O. Gires, M. Ueffing, W. Kolch, and W. Hammerschmidt.** 1997. Epstein-Barr virus latent membrane protein-1 triggers AP-1 activity via the c-Jun N-terminal kinase cascade. EMBO J. **16:**6478–6485.
34. **Kinchington, P., and J. I. Cohen.** 2000. Varicella-zoster virus proteins, p. 556. *In* A. M. Arvin and A. A. Gershon (ed.), Varicella-zoster virus: virology and clinical management, 1st ed. Cambridge University Press, Cambridge, United Kingdom.
35. **Kinchington, P., G. Inchauspe, J. H. Subak-Sharpe, F. Robey, J. Hay, and W. T. Ruyechan.** 1988. Identification and characterization of a varicella-

zoster virus DNA-binding protein by using antisera directed against a predicted synthetic oligopeptide. J. Virol. **62:**802–809.

36. **Kinchington, P. R., D. Bookey, and S. E. Turse.** 1995. The transcriptional regulatory proteins encoded by varicella-zoster virus open reading frames (ORFs) 4 and 63, but not ORF 61, are associated with purified virus particles. J. Virol. **69:**4274–4282.

37. **Kinchington, P. R., K. Fite, A. Seman, and S. E. Turse.** 2001. Virion association of IE62, the varicella-zoster virus (VZV) major transcriptional regulatory protein, requires expression of the VZV open reading frame 66 protein kinase. J. Virol. **75:**9106–9113.

38. **Kinchington, P. R., K. Fite, and S. E. Turse.** 2000. Nuclear accumulation of IE62, the varicella-zoster virus (VZV) major transcriptional regulatory protein, is inhibited by phosphorylation mediated by the VZV open reading frame 66 protein kinase. J. Virol. **74:**2265–2277.

39. **Kinchington, P. R., J. K. Hougland, A. M. Arvin, W. T. Ruyechan, and J. Hay.** 1992. The varicella-zoster virus immediate-early protein IE62 is a major component of virus particles. J. Virol. **66:**359–366.

40. **Kinchington, P. R., and S. E. Turse.** 1998. Regulated nuclear localization of the varicella-zoster virus major regulatory protein, IE62. J. Infect. Dis. **178:**S16–S21.

41. **Kyriakis, J. M., and J. Avruch.** 2001. Mammalian mitogen-activated protein kinase signal transduction pathways activated by stress and inflammation. Physiol. Rev. **81:**807–859.

42. **Kyriakis, J. M., P. Banerjee, E. Nikolakaki, T. Dai, E. A. Rubie, M. F. Ahmad, J. Avruch, and J. R. Woodgett.** 1994. The stress-activated protein kinase subfamily of c-Jun kinases. Nature **369:**156–160.

43. **Lawler, S., Y. Fleming, M. Goedert, and P. Cohen.** 1998. Synergistic activation of SAPK1/JNK1 by two MAP kinase kinases in vitro. Curr. Biol. **8:**1387–1390.

44. **Leisenfelder, S. A., and J. F. Moffat.** 2006. Varicella-zoster infection of human foreskin fibroblast cells results in atypical cyclin expression and cyclin-dependent kinase activity. J. Virol. **80:**5577–5587.

45. **Litwin, V., W. Jackson, and C. Grose.** 1992. Receptor properties of two varicella-zoster virus glycoproteins, gpI and gpIV, homologous to herpes simplex virus gE and gI. J. Virol. **66:**3643–3651.

46. **Ludwig, S., S. Pleschka, and T. Wolff.** 2003. Influenza-virus-induced signaling cascades: targets for antiviral therapy? Trends Mol. Med. **9:**46–52.

47. **MacCorkle, R. A., and T.-H. Tan.** 2005. Mitogen-activated protein kinases in cell-cycle control. Cell Biochem. Biophys. **43:**451–461.

48. **Manning, A. M., and R. J. Davis.** 2003. Targeting JNK for therapeutic benefit: from junk to gold? Nature **2:**554–565.

49. **McLean, T. I., and S. L. Bachenheimer.** 1999. Activation of c-Jun N-terminal kinase by herpes simplex virus type 1 enhances viral replication. J. Virol. **73:**8415–8426.

50. **Minden, A., A. Lin, F.-X. Claret, A. Abo, and M. Karin.** 1995. Selective activation of the JNK signaling cascade and c-Jun transcriptional activity by the small GTPases and Cdc42Hs. Cell **81:**1147–1157.

51. **Moffat, J. F., M. A. McMichael, S. A. Leisenfelder, and S. L. Taylor.** 2004. Viral and cellular kinases are potential antiviral targets and have a central role in varicella zoster virus pathogenesis. Biochim. Biophys. Acta **1697:**225–231.

52. **Morrison, D. K., and R. J. Davis.** 2003. Regulation of MAP kinase signaling modules by scaffold proteins in mammals. Annu. Rev. Cell Dev. Biol. **19:**91–118.

53. **Narayanan, A., M. L. Noguiera, W. T. Ruyechan, and T. M. Kristie.** 2005. Combinatorial transcription of herpes simplex virus and varicella zoster virus immediate early genes is strictly determined by the cellular coactivator HCF-1. J. Biol. Chem. **280:**1369–1375.

54. **Niizuma, T., L. Zerboni, M. H. Sommer, H. Ito, S. Hinchcliffe, and A. M. Arvin.** 2003. Construction of varicella-zoster virus recombinants from parent Oka cosmids and demonstration that ORF 65 protein is dispensable for infection of human skin and T cells in the SCID-hu mouse model. J. Virol. **77:**6062–6065.

55. **Pan, H., J. Xie, F. Ye, and S.-J. Gao.** 2006. Modulation of Kaposi's sarcoma-associated herpesvirus infection and replication by MEK/ERK, JNK, and p38 multiple mitogen-activated protein kinase pathways during primary infection. J. Virol. **80:**5371–5382.

56. **Panteva, M., H. Korkaya, and S. Jameel.** 2003. Hepatitis viruses and the MAPK pathway: is this a survival strategy? Virus Res. **92:**131–140.

57. **Peng, H., H. He, J. Hay, and W. T. Ruyechan.** 2003. Interaction between the varicella zoster virus IE62 major transactivator and cellular transcription factor Sp1. J. Biol. Chem. **278:**38068–38075.

58. **Perkins, D., K. A. Gyure, E. F. Pereira, and L. Aurelian.** 2003. Herpes simplex virus type 1-induced encephalitis has an apoptotic component associated with activation of c-Jun N-terminal kinase. J. Neurovirol. **9:**101–111.

59. **Qi, M., and E. A. Elion.** 2005. MAP kinase pathways. J. Cell Sci. **118:**3569–3572.

60. **Rahaus, M., N. Desloges, M. Yang, W. T. Ruyechan, and M. H. Wolff.** 2003. Transcription factor USF, expressed during the entire phase of varicella-zoster virus infection, interacts physically with the major viral transactivator IE62 and plays a significant role in virus replication. J. Gen. Virol. **84:**2957–2967.

61. **Rahaus, M., N. Desloges, and M. H. Wolff.** 2005. ORF 61 protein of varicella-zoster virus influences JNK/SAPK and p38/MAPK phosphorylation. J. Med. Virol. **76:**424–433.

62. **Rahaus, M., N. Desloges, and M. H. Wolff.** 2004. Replication of varicella-zoster virus is influenced by the levels of JNK/SAPK and p38/MAPK activation. J. Gen. Virol. **85:**3529–3540.

63. **Rahaus, M., and M. H. Wolff.** 2000. Transcription factor Sp1 is involved in the regulation of varicella-zoster virus glycoprotein E. Virus Res. **69:**69–81.

64. **Rahaus, M., and M. H. Wolff.** 2003. Reciprocal effects of varicella-zoster virus (VZV) and AP1: activation of jun, fos and ATF-2 after VZV infection and their importance for the regulation of viral genes. Virus Res. **92:**9–21.

65. **Rodriguez, J. E., T. Moninger, and C. Grose.** 1993. Entry and egress of varicella virus blocked by same anti-gH monoclonal antibody. Virology **196:**840–844.

66. **Roovers, K., and R. K. Assoian.** 2000. Integrating the MAP kinase signal into the G$_1$ phase cell cycle machinery. Bioessays **22:**818–826.

67. **Santibanez, J. F., and C. Hurtado.** 2005. Ha-Ras sensitizes transformed mouse skin cells to anisomycin-induced apoptosis. FEBS Lett. **579:**6459–6464.

68. **Taylor, S. L., P. R. Kinchington, A. Brooks, and J. F. Moffat.** 2004. Roscovitine, a cyclin-dependent kinase inhibitor, prevents replication of varicella-zoster virus. J. Virol. **78:**2853–2862.

69. **Theodosiou, A., and A. Ashworth.** 2002. MAP kinase phosphatases. Genome Biol. **3:**REVIEWS3009.

70. **Wang, G., J. W. Barrett, M. Stanford, S. J. Werden, J. B. Johnston, X. Gao, M. Sun, J. Q. Cheng, and G. McFadden.** 2006. Infection of human cancer cells with myxoma virus requires Akt activation via interaction with a viral ankyrin-repeat host range factor. Proc. Natl. Acad. Sci. USA **103:**4640–4645.

71. **Whitmarsh, A. J., and R. J. Davis.** 2001. Analyzing JNK and p38 mitogen-activated protein kinase activity. Methods Enzymol. **332:**319–336.

72. **Xia, Y., and M. Karin.** 2004. The control of cell motility and epithelial morphogenesis by Jun kinases. Trends Cell Biol. **14:**94–101.

73. **Yao, F., and R. J. Courtney.** 1989. A major transcriptional regulatory protein (ICP4) of herpes simplex virus type 1 is associated with purified virions. J. Virol. **63:**3338–3344.

74. **Zachos, G., B. Clements, and J. Conner.** 1999. Herpes simplex virus type 1 infection stimulates p38/c-Jun N-terminal mitogen-activated protein kinase pathways and activates transcription factor AP-1. J. Biol. Chem. **274:**5097–5103.